SAND2010-1089C

Design of RF MEMS Switches without Pull-in Instability

W. Cyrus Proctor[a], Gregory P. Richards[b], Chongyi Shen[c], Tyler Skorczewski[d], Min Wang[e], Jingyan Zhang[f], Peng Zhong[g], Jordan E. Massad[h], Ralph Smith[i]

[a]North Carolina State University, [b]Kent State University, [c]University of Iowa, [d]University of California Davis, [e]Northern Illinois University, [f]Penn State University, [g]University of Tennessee Knoxville, [h]Sandia National Laboratories, [i]North Carolina State University

ABSTRACT

Micro-electro-mechanical systems (MEMS) switches for radio-frequency (RF) signals have certain advantages over solid-state switches, such as lower insertion loss, higher isolation, and lower static power dissipation. Mechanical dynamics can be a determining factor for the reliability of RF MEMS. The RF MEMS ohmic switch discussed in this paper consists of a plate suspended over an actuation pad by four double-cantilever springs. Closing the switch with a simple step actuation voltage typically causes the plate to rebound from its electrical contacts. The rebound interrupts the signal continuity and degrades the performance, reliability and durability of the switch. The switching dynamics are complicated by a nonlinear, electrostatic pull-in instability that causes high accelerations. Slow actuation and tailored voltage control signals can mitigate switch bouncing and effects of the pull-in instability; however, slow switching speed and overly-complex input signals can significantly penalize overall system-level performance. Examination of a balanced and optimized alternative switching solution is sought. A step toward one solution is to consider a pull-in-free switch design. In this paper, determine how simple RC-circuit drive signals and particular structural properties influence the mechanical dynamics of an RF MEMS switch designed without a pull-in instability. The approach is to develop a validated modeling capability and subsequently study switch behavior for variable drive signals and switch design parameters. In support of project development, specifiable design parameters and constraints will be provided. Moreover, transient data of RF MEMS switches from laser Doppler velocimetry will be provided for model validation tasks. Analysis showed that a RF MEMS switch could feasibly be designed with a single pulse waveform and no pull-in instability and achieve comparable results to previous waveform designs. The switch design could reliably close in a timely manner, with small contact velocity, usually with little to no rebound even when considering manufacturing variability.

1. INTRODUCTION AND MOTIVATION

Micro-electro-mechanical systems (MEMS)[1] have been used in various radio frequency (RF) applications to improve operation and performance.[2–5] RF MEMS ohmic switches have shown lower insertion loss, higher isolation, greater linearity, and lower static power dissipation than solid state switches.[2] Mechanical dynamics can be a determining factor for the reliability of RF MEMS. The RF MEMS ohmic switch discussed in this paper consists of a plate, suspended over an actuation pad by four double-cantilever springs as depicted in Figure 1. During operation, an input voltage is typically applied to close an RF MEMS switch, and the dynamics of the closure event have a significant impact on the performance and design lifetime of a switch.

The kinetic energy of a switch scales with its velocity and when a switch closes this energy must be dissipated before the switch attains a stable, closed state. This was observed experimentally using laser-Doppler vibrometry, where a switch was shown to bounce on its contacts a number of times before closing.[7] The voltage signal used to close the switch was then replaced with a sequence of pulses that was shown to greatly reduce the velocity with which the switch impacted its electrical contacts and the subsequent bouncing. A high velocity before impact can also lead to higher deformations and hence, higher stresses in the device during the close event. These observations motivate the use of shaped voltage waveforms to limit the contact velocities of electrostatically actuated MEMS devices.

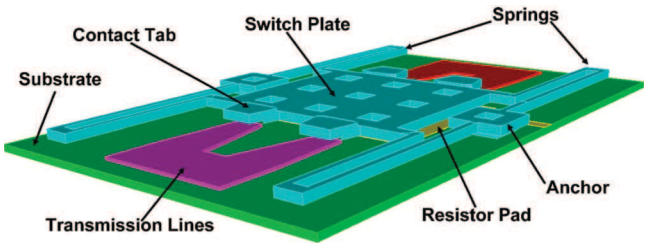

Figure 1. Three dimensional RF-MEMS switch.[6]

There are many ways to design the waveform of the input voltage. In this paper, we focus on one pulse to close the switch and hold it in contact. Moreover, the work described in this paper seeks to model and optimize the dynamics of an RF MEMS switch while accounting for the unit-to-unit variability inherent in the fabrication of the switches.

2. MODEL EQUATIONS

Using standard reduction techniques, a single-degree-of-freedom model of the switch was constructed.[8] Most of the relevant physics of the free system could be quantified using a forced, damped harmonic oscillator. The equation for this model is

$$\ddot{x} + 2\zeta_o\omega_o\dot{x} + \omega_o^2 x = \frac{F_e}{m_{eff}} \tag{1}$$

where x the position of the switch plate mass from equilibrium, m_{eff} is the effective mass of the plate-spring structure, ζ_o is the dampening coefficient, ω_o is the natural frequency of the spring system. F_e is the electrostatic force exerted on the plate defined by

$$\frac{F_e}{m_{eff}} = \frac{\alpha V(t)^2}{(g-x)^2} \tag{2}$$

with

$$\alpha = \frac{\epsilon A}{2m_{eff}}.$$

Here g is the gap thickness between the plate and electrode at equilibrium, d_t is the distance that the switch travels between equlibrium and the waveguides, where ϵ is the permittivity of air, A is the cross-sectional area of the switch plate, $V(t)$ is the applied voltage. Substituting this into Eq.(1) yields

$$\ddot{x} + 2\zeta_o\omega_o\dot{x} + \omega_o^2 x = \frac{\alpha V(t)^2}{(g-x)^2}. \tag{3}$$

This system accurately describes the switch dynamics when the switch is not in contact with the waveguides. Oscillation of the switch plate during contact in the closed position can approximately be quantified by switching to new values for the natural frequency and damping of the system, $\omega_o \rightarrow \omega_c$ and $\zeta_o \rightarrow \zeta_c$, respectively. The dynamics of the switch when in contact with the waveguides is then

$$\ddot{x} + 2\zeta_c\omega_c\dot{x} + \omega_c^2 x = \frac{\alpha V_h(t)^2}{(g-x)^2}. \tag{4}$$

Experimental data is used to find values for ζ_c and ω_c. Using laser-Doppler vibrometry, the position of an actuated plate over time is can be recorded. This data can then be used to perform a least squares

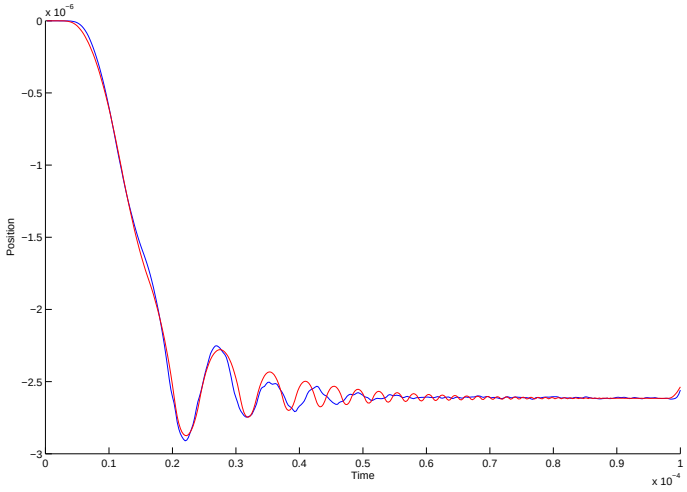

Figure 2. Model calibration for closing switch data from.[8]

fit to determine the appropriate values of ζ_c and ω_c. The resulting values are found to be $\zeta_c = 0.38$ and $\omega_c = 365.05$ kHz. Figure 2, illustrates the fit between the experimental data and a numerical solution to the system under the same conditions with the best fit values for ζ_c and ω_c. We see very good agreement for the first several contacts of the switch. As the switch continues to bounce off the waveguides, we hypothesize higher-order effects account for the discrepancy between the one dimensional model and the experimental data.

3. DETERMINISTIC ANALYSIS

Our goal is to design an optimized RF MEMS switch that does not suffer from the negative effects of switch bounce on contact with the waveguides but still closes very quickly. We first consider a deterministic optimization for the design of the MEMS switch. This optimization will allow insight into the behaviour of the system with a variety of conditions. Additionally, this analysis along with sensitivity analysis will give some intuition regarding which parameters are most important for the ultimate goal of optimizing switch parameters under uncertainty. We choose the waveform of the applied voltage as one that can be easily achieved by a RC circuit, thus we provide the solvers with a voltage curve that can be determined by two parameters.

$$V_h(t) = \begin{cases} V_{hold}\left(1 - e^{(t/t_b)}\right) & V_h(t) < 0.99 * V_{hold} \\ V_{hold} & \text{otherwise} \end{cases} \tag{5}$$

To optimize, we calculate an objective function from the numerical solutions to the model equations (1) and (5). The objective function to minimize is chosen as the energy of the system between the time of first contact and the time the switch is considered closed. This function contains measures of the time it takes to close the switch and contact velocities of the switch, which is directly related to impact energies. This function is expressed as

$$F = \int_{t_{contact}}^{t_{close}} \dot{x}^2(t)dt. \tag{6}$$

Here t_{close} is defined by the point in time in which the contact tabs on the switch plate come in 'good contact' with the transmission lines and stay within a defined tolerance. The point of 'good isolation' for the switch

Table 1. Selected deterministic optimization results. Optimization results setting a fixed travel distance d_t, and using equation (6) as the metric. Here g is the gap distance, V_h is the holding voltage, t_b build up time constant, ω_o is the natural frequency of the system, cv is the contact velocity, t_{close} is the time to close the switch, and en is the energy from first contact to switch closure.

$d_t(m)$	$g(m)$	$V_h(V)$	$t_b(s)$	$\omega_o(Hz)$	$cv(m/s)$	$t_{close}(s)$	$en\ (m^2/s)$
1.2e-6	3.6e-6	149.1	3.0e-7	1.5e5	0.28	8.3e-5	3.1e-7
9.7e-7	2.9e-6	131.1	3.4e-7	1.6e5	0.29	4.8e-5	1.9e-7
7.4e-7	2.2e-6	85.9	4.1e-7	1.6e5	0.22	4.9e-5	1.1e-7
5.1e-7	1.5e-6	51.3	7.4e-7	1.6e5	0.16	4.1e-5	5.1e-8
2.8e-7	1.6e-6	45.1	7.8e-7	1.6e5	0.09	4.5e-5	2.1e-8
6.3e-8	2.0e-6	30.4	1.1e-6	1.6e5	0.02	3.2e-5	1.1e-9

was defined by capacitance of 170e-18 Farads, which corresponds to 52.08 nm. 'Good contact' was assumed to be 10 times less distance than the defined tolerance for 'good isolation'.

We optimize several parameters in our system. They are the travel distance d_t, the gap thickness g, the holding voltage V_h, the voltage build up time constant t_b, and the natural frequency of the (open) system ω_o. To find the optimization of our objective function, we use MATLAB's built in optimization tool, `fminsearch()`. When using `fminsearch()` we adjust our objective function slightly by adding in a penalty term for when the test parameters are outside of the physical bounds of the system.

Analysing the results of several runs, we observe that the optimization routine always returns an optimal travel distance that is equal to the minimum travel distance allowed. Thus we refine our search to optimize only over g, V_h, t_b and ω_o. Some results of these searches are compiled in Table 1 for various choices of d_t.

These results show several interesting facts about the behaviour of the optimized system as a function of the travel distance. Both the optimal hold voltage and the build up time constant seem to have a near linear relation to travel distance. Additionally, the optimal natural frequency of the system changes very little across all optimization computations.

4. NUMERICAL SENSITIVITY ANALYSIS

It is important to check how sensitive the computed solutions of the model are to the choice of input parameter values. Parameters used in the model of MEMS switch dynamics will vary during manufacturing, and any voltage waveform designed to close the switch should be effective over a range of values defined by the tolerances of fabrication. Before we undergo an uncertainty analysis of the model, we first identify which parameters of the model are the most sensitive. Sensitivity here is checked through direct simulations where all parameters except the parameter of interest are held constant at an optimal value. Several computations are performed where the parameter of interest is varied across an interval determined from experience with manufacturing and previous simulations. These values are shown in Table 2. Extracted from the simulations are the time it takes to close the switch and the largest impact velocity the plate makes with the waveguides. One can infer sensitivity from the relationships between these two variables and the parameter of interest. Parameters with the greatest sensitivity are considered in the uncertainty quantification study.

The results of these simulations show that the relationships between impact velocity and several parameters are largely linear; see Figure 3. We can therefore quantify the sensitivity

$$S = \frac{\frac{\Delta R}{R_{opt}}}{\frac{\Delta \sigma}{\sigma_{opt}}} \tag{7}$$

as the magnitude of the slope of the line fitting a plot of scaled impact velocity and scaled parameter values. Equation (7) outlines a generalized definition of sensitivity, S, of the normalized change in output response $\Delta R = R - R_{opt}$ due to the change in normalized input $\Delta\sigma = \sigma - \sigma_{opt}$. These results are shown in Table 3.

Table 2. Parameters investigated in sensitivity analysis

Parameter	Optimal Value	Min Value	Max Value
d_t [m]	5.00e-07	5.00e-07	1.13e-06 ($g_{opt}/3$)
g [m]	3.41e-06	1.50e-06	4.00e-04
V_h [V]	1.27e+02	5.00e+01	1.5e+02
t_b [s]	3.06e-07	1.00e-07	1.00e-04
ω_o [Hz]	1.49e+05	1.12e+05 (75% ω_o)	1.86e+05 (125% ω_o)
$x(0)$ [m]	0.00e+00	-1.00e-07 (-20% d_{opt})	1.00e-07 ($+20\%$ d_{opt})
$\dot{x}(0)$ [m/s]	0.00e+00	-1.55e-02 (-10% vc_{opt})	1.55e-02 ($+10\%$ vc_{opt})

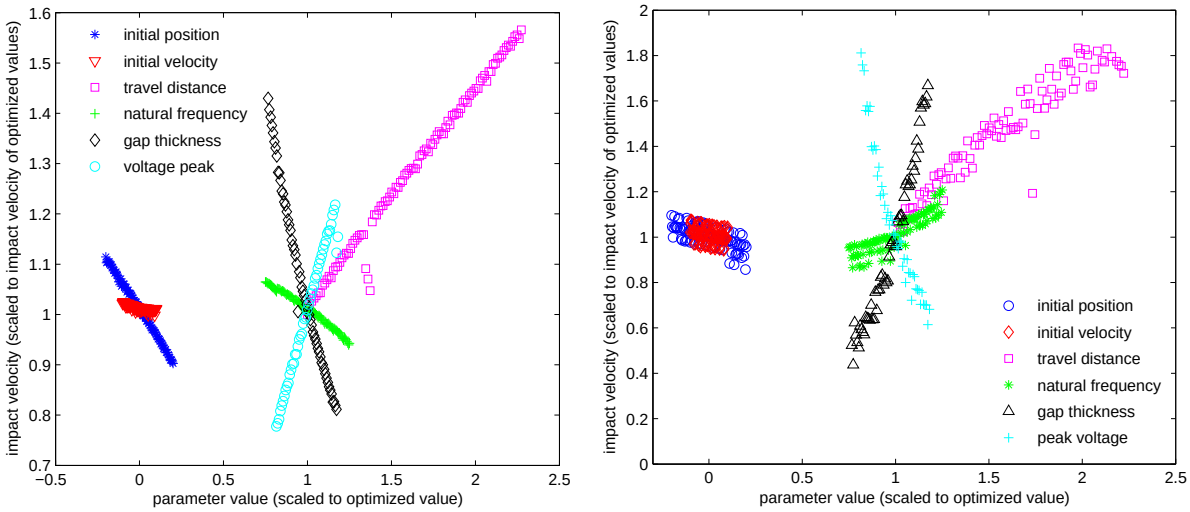

Figure 3. Sensitivity of model parameters. Shown are plots of impact velocity (left) and closing time (right) scaled to their optimum values versus parameter values scaled to optimized values. For initial velocity and initial displacement the parameter values are scaled to the impact velocity with optimized values and optimized travel distance, respectively. Larger slopes indicate more sensitivity.

From these results, we see that impact velocity is most sensitive to changes in the gap thickness, peak voltage, initial displacement, and travel distance. It is moderately sensitive to natural frequency and not sensitive to changes in initial velocity or voltage ramp up time.

The same analysis also applied to the time it takes to close the switch. The results of the scaled closing

Table 3. Quantification of impact velocity sensitivity of model parameters

impact velocity analysis		closing time analysis	
Parameter	Sensitivity	Parameter	Sensitivity
d_t	0.44	d_t	0.64
g	1.5	g	2.8
V_h	1.2	V_h	2.9
t_b	≈ 0	t_b	≈ 0
ω_o	0.24	ω_o	0.49
$x(0)$	0.51	$x(0)$	0.27
$\dot{x}(0)$	0.075	$\dot{x}(0)$	0.16

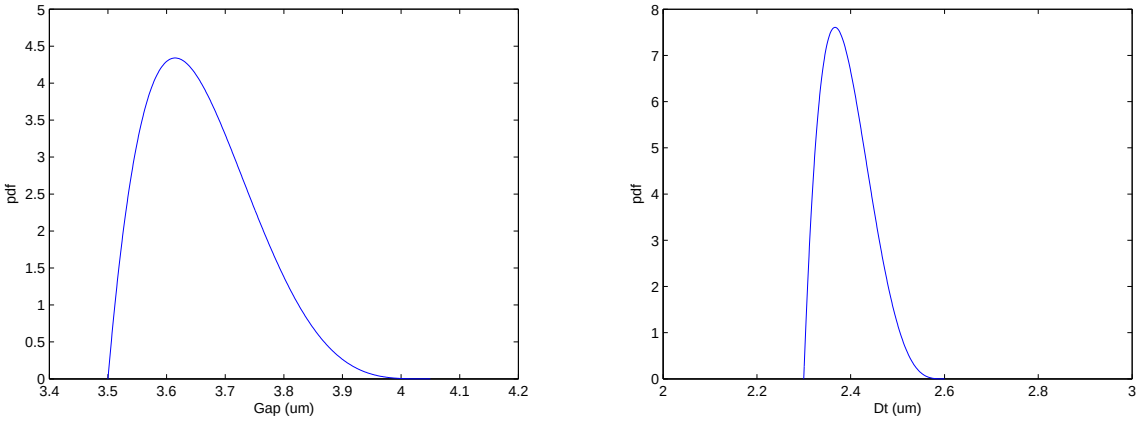

Figure 4. Distributions of gap and d_t after parameter estimation.

time versus scaled parameter value plots again look linear, though this relationship is less well defined; see Figure 3. Again sensitivity is quantified as the magnitude of the slope of the linear fit to the data. The results shown in Table 3 show that switch closing time is most sensitive to peak voltage and gap thickness. These are followed by travel distance, natural frequency, and initial position. Closing time is least sensitive to initial velocity and the voltage ramp up time constant, as with impact velocity.

5. UNCERTAINTY QUANTIFICATION

From the deterministic optimization, we have a set of device parameters that are considered to be optimized. However, these parameters are for one single switch. While in mass production, one must also consider random unit-to-unit variability between the switches due to manufacturing techniques. Namely, it is that even if we target the gap at 3.5μ m for every single switch (for example), their actual gaps may be 3.4μm, 3.6μm, etc. The same variability could apply to travel distance, K_{eff}, and m_{eff}.

Our existing data of past experiments and relevant analysis suggest that a waveform designed to optimize one switch cannot give good results when applied to an ensemble of switches with more than 1,000 variations. This is due to the existence of variability mentioned previously and because these statistics have not been incorporated in the design. Uncertainty analysis aims to provide a waveform to an ensemble of switches so that the overall performance of a batch of switches is optimized. This waveform is potentially different than the one designed for one specific switch.

From the sensitivity analysis, we notice that ω_o is not very sensitive to our optimization. As such, we exclude ω_o in the uncertainty analysis. Similarly, we will not consider the variability of K_{eff} and m_{eff}, which both are linked to ω_o. Here we consider variations in initial displacement, gap and travel distance.

The distribution of these random variables needs to be specified before we perform an uncertainty analysis. Previous experimental measurements indicated that a generalized Beta distribution is appropriate and conservative for both g and d_t,[6] with α and β parameters 2.0 and 4.8 for g, respectively; for d_t they are 2.0 and 4.5, respectively. We assume a uniform distribution for the initial displacement.

We consider three scenarios based upon varying choices for the expected value of the travel distance d_t. We denote these scenarios as low, medium, and high and values for the expected value of d_t and g are given in Table 5. For each scenario, 25 samples are taken from each of the parameter distributions which form a total of $25^3 = 15625$ simulations. We first consider the contact velocity histogram without considering unit-to-unit variability and make a series of observations to serve as a base with which to compare later. In the medium travel distance scenario, up to $6967/15625 = 45\%$ of the switches fail to close. This is due to the travel distance d_t, is close to the distance where the pull-in instability occurs, $g/3$. Variations in d_t and

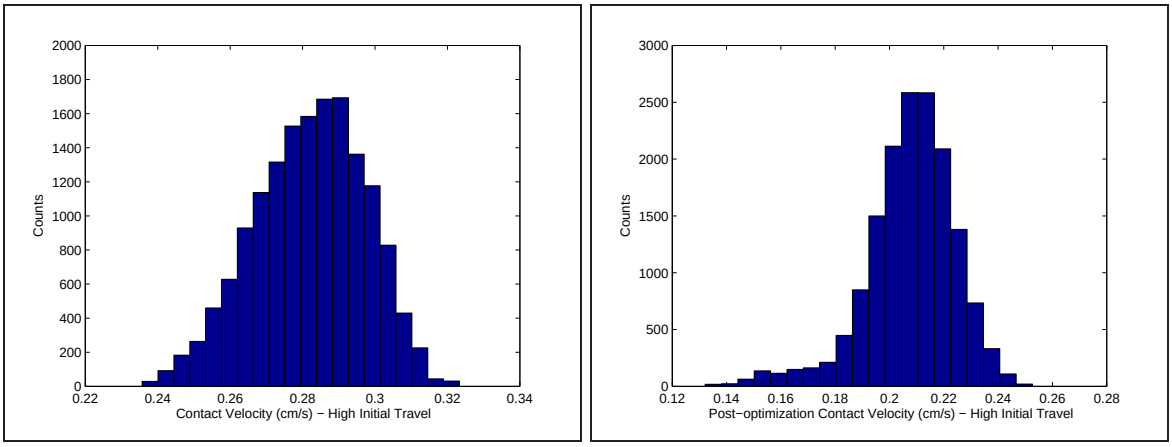

Figure 5. Comparison of optimized values before (left) and after (right) uncertainty analysis using contact velocity as objective function.

g will cause some switches to operate with the pull in instability, which alters switch dyanmics significantly. In the high travel distance scenario, almost no switch closes with a speed less than 25 cm/s. We present this result to illustrate the issue when we ignore the unit-to-unit variability among the devices, and for a comparison purpose how better we can make with including random variability.

Next, we admit the existence of unit-to-unit variability and design the waveform so that optimized overall performance is achieved. The optimization process we use is to minimize the 90th percentile of contact velocity v_{90}, which is defined by

$$P(v > v_{90}) = 0.1.$$

For these optimizations, we only allow the parameters of the voltage waveform to change and not the physical device parameters (d_t, g, ω_o) We still consider the three low, medium and high scenarios and results of this optimization are shown in Table 5 along with the results from the deterministic optimizations. Figure 5 shows how the distribution of contact velocities change between the deterministic case and the case with uncertainty for the high travel distance scenario.

Improvement is obvious when uncertainty is included in the analysis. In the medium travel distance scenario, the switch fail rate drops rapidly from 45% to about 15%. In the high travel distance scenario, even from visual comparison, one can easily perceive the effect of optimization. From a statistical perspective, it is also not hard to show that the improvement observed is quite significant. To be specific, we calculate an asymptotic 95% confidence interval for the deterministic model's contact velocities and also for the probability models. Since the distribution of contact velocity is not known, we use $\bar{v} \pm 1.96 \times \sqrt{Sv^2/N}$ to calculate the asymptotic 95% interval. As such, we get the interval for deterministic model is (0.2521, 0.3119), while for the probability model is (0.1752,0.2402). These ranges have absolutely no overlap with each other. This is strong evidence when performing an optimization it is necessary to consider uncertainty in model parameters.

Table 4. Comparison of waveform designs between deterministic model and uncertainty model.

Scenario (based on d_t):	V_h**(Deter)**	t_b**(Deter)**	V_h**(Uncer)**	t_b**(Uncer)**	$E(g)$	$E(d_t)$
Low	41.303	8.1655e-7	38.403	8.4693e-7	1.31e-6	1.668e-7
Medium	51.309	7.4383e-7	49.385	7.9032e-7	1.5338e-6	5.112e-7
High	149.11	3.0068e-7	124.95	3.3256e-7	3.6037e-6	1.2e-6

Design Optimization

In this section, we study how the change of parameter distribution effects the optimized result. We start from shifting the support of the distributions of parameters and investigate the generated pdf histograms of optimized contact velocity, closing time, and energy. Following each distribution of g, d_t, and x_0, 10 random values are generated for each parameter, respectively, giving us totally $1,000 = 10^3$ samples. Thus, we get a corresponding distribution set of contact velocities, closing times, and energies from those 1000 samples. The goal is to pick up a shift value which provides a 'best' optimized distribution set.

The objective function to be minimized is

$$J(\epsilon) = V_p + c_1 p_f,$$

where ϵ denotes the shift of distribution set, V_p denotes the 90 percentile of the optimized contact velocity distribution, p_f denotes the probability that the switch fails to close, and c_1 is a weight to balance the energy and the number of switches which fails to close.[8]

In the computational routine, the shift of distribution is characterized by the variation of expectation value. Since the deterministic model provides several sets of optimal parameters, the uncertainty analysis is performed within three different parameter domains distinguished by the value of travel distance d_t. We elect the three different d_t values from the low, medium and high scenarios investiaged earlier to be the initial expectation values of travel distance distributions. We do separate iterations for each to obtain three sets of optimized results. The small initial d_t value provides the best results. The histograms for optimized distribution of contact velocity, energy and closing time for this case are shown in Figure 6. The final parameters optimized under uncertainty are given in Table 5.

Table 5. Waveform and distribution design under uncertainty.

Optimized Values:	V_h	t_b	$E(d_t)$	$E(g)$
Small Initial	40.34	8.13e-7	1.68e-7	1.81e-6
Medium Initial	45.7	7.78e-7	4.63e-7	1.81e-6
Large Initial	135.4	3.05e-7	1.20e-6	3.85e-6

6. CONCLUSION

In this paper, we discuss a one dimensional forced damped harmonic oscillator model governing the dynamics of an RF MEMS switch. We have fit model parameters from experimental data to account for contact dynamics. Through sensitivity analyses, we determine that gap, peak voltage and initial distance are sensitive model parameters that can significantly affect model output such as switch closing time and contact velocity. Parameters such as initial velocity and natural frequency are less sensitive. It is important to note that while model output is not sensitive to natural frequency, this parameter may play an important role in switch opening dynamics. Exploring this is left to future work. Once the sensitive model parameters are determined, we optimize the the voltage waveform over given distributions of the sensitive variables to perform an uncertainty analysis. This optimization returns a peak voltage and an RC time constant so the switch can be driven with a simple RC circuit voltage waveform. We also find it is possible to design a MEMS switch that closes without rebounding.

Through the results obtained from this project we can make several recommendations to the manufacturers of RF MEMS switches. The first is to use the smallest travel distance possible to make the switch with reliability. Smaller travel distances require smaller gap thicknesses and peak voltages to drive. We also recommend to use smaller RC time constants in conjunction with peak voltages, as these optimize model output. The final recommendation is to develop manufacturing processes that reduce variability in gap thickness and travel distance as these will produce more reliable switch dynamics and output.

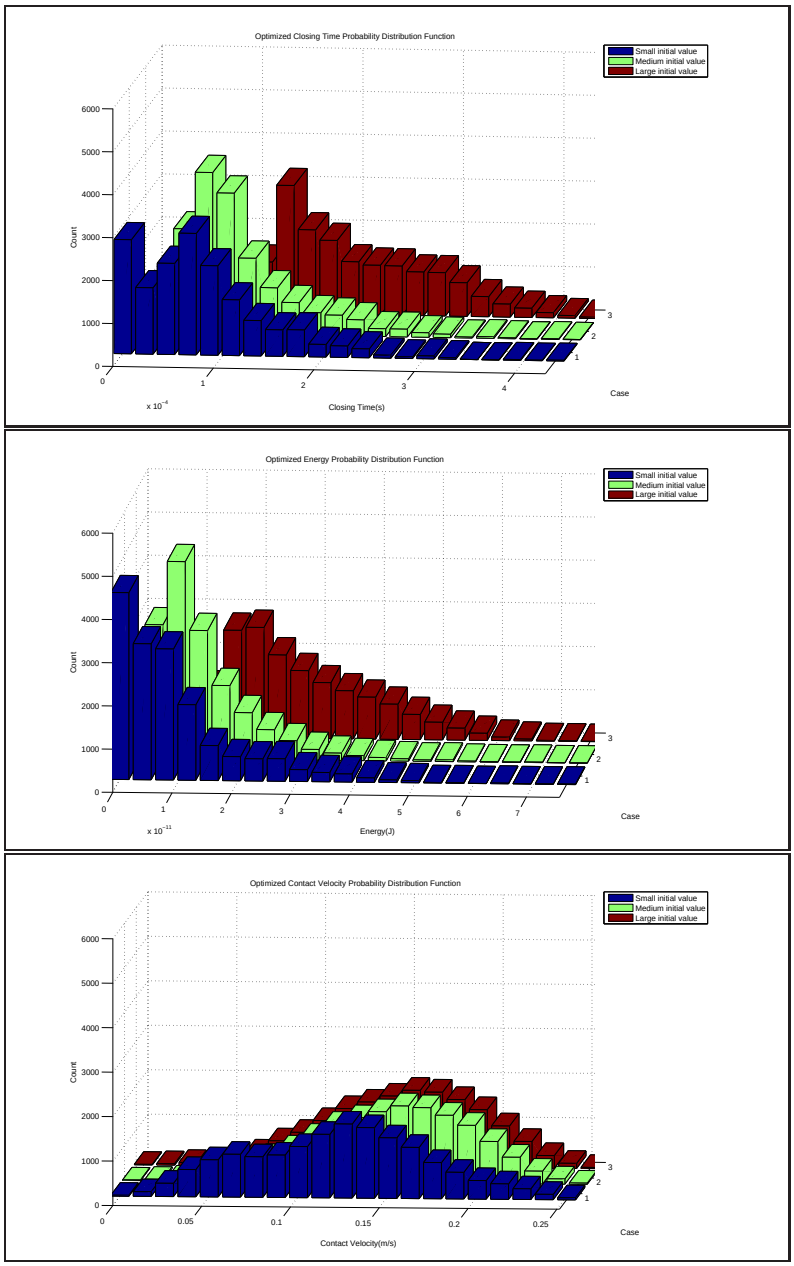

Figure 6. Uncertainty optimized responses using contact velocity objective function. Histograms of closing times (top), energies (middle) and contact velocities (bottom) for each of the low (blue), medium (green) and high (red) travel distance scenarios.

ACKNOWLEDGMENTS

This work was part of the Industrial Mathematical and Statistical Modeling Workshop held at North Carolina State University July 20-28, 2009. The workshop is funded in part by the Statistical and Applied Mathematical Sciences Institute (SAMSI). Sandia is a multiprogram laboratory operated by Sandia Corporation, a Lockheed Martin Company, for the United States Department of Energy under contract DE-AC04-94AL85000.

REFERENCES

[1] Petersen, K. E., "Silicon as a mechanical material," *IEEE* **70**, 420–457 (May 1982).

[2] Yao, J. J., "RF MEMS from a device perspective," *Journal of Micromechanics and Microengineering* **10**, R9–R38 (2000).

[3] Lucyszyn, S., "Review of radio frequency microelectromechanical systems technology," *Science, Measurement and Technology, IEEE Proceedings* **151**, 93–103 (March 2004).

[4] Nguyem, C. T. C., Katehi, L. P. B., and Rebeiz, G. M., "Micromachined devices for wireless communications," *IEEE* **86**, 1756–1768 (August 1998).

[5] Rebeiz, G. M., [*RF MEMS Theory, Design and Technology*], Wiley (2003).

[6] Allen, M., Massad, J., Field, R. J., and Dyck, C., "Input and design optimization under uncertainty to minimize the impact velocity of an electrostatically actuated mems switch," *Journal of Vibration and Acoustics* **130** (2008).

[7] Sumali, H., Massad, J., Czaplewski, D., and Dyck, C., "Waveform design for pulse-and-hold electrostatic acuation in mems," *Sensors and Actuators A* **134**, 213–220 (2007).

[8] Blecke, J., Epp, D., Sumali, H., and Parker, G., "A simple learning control to eliminate rf-mems switch bounce," *Journal of Microelectromechanical Systems* **18**, 458–465 (2009).